Aqib et al.
Journal of Engineering and Applied Science (2023) 70:20
https://doi.org/10.1186/s44147-023-00188-7

Journal of Engineering and Applied Science

RESEARCH **Open Access**

Experimental and numerical analysis of rainfall-induced slope failure of railway embankment of semi high-speed trains

Mohammad Aqib[1], Shadab Usmani[2], Tanveer Khan[3], Md Rehan Sadique[1*] and Mohd Masroor Alam[1]

*Correspondence: rehan.sadique@gmail.com; rehan.sadique@zhcet.ac.in

[1] Department of Civil Engineering, Aligarh Muslim University, Aligarh 202002, India
[2] Department of Building, Civil and Environmental Engineering, Concordia University, Montreal, Canada
[3] Ministry of Railways, IRSE, New Delhi, India

Abstract

Safety and maintenance of railway tracks has been very crucial, for sustainable economic development of many nations. Almost the entire Indian railway tracks were built over the raised earth embankments. These embankments are susceptible to slope failure due to numerous reasons. One of the major cause is seepage and surface runoff during rainy (monsoon) season. Erosion by gullying has regarded as most significant failure scar. Various researches had studied the embankment failure due to rainfall. However, the gullying effect on the slope failure has been missing in these studies. Hence, in this study slope stability analysis of the railway embankment has been performed considering the gullying. Embankment of Dedicated Freight Corridor (India) has been taken up in this study. The present study has three sections (a) Field observation, (b) scaled laboratory modelling, and (c) FEM-based numerical analysis. The effect of vegetation, degree of compaction, and the intensity of rainfall on the slope stability has been evaluated. Effect of gullying has incorporated through change in shape and dimension of embankment. It has been found that vegetation significantly reduced the gully formation and also the less compacted slope experienced more gullies formation as compared to the more compacted slope. While varying the rainfall intensity from 20 to 100 mm, it has been observed that without consideration of gully higher FOS (factor of safety) was reported. Moreover, FOS decrease with increase of rainfall from 20 to 100 mm and becomes constant after that.

Keywords: Slope stability, Rain-induced failure, Earth embankments, Physical model, Simulation

Introduction

Slope failure is one of the most common issues in geotechnical engineering caused by natural processes or anthropogenic intervention. In hilly tracts, large slope failures with deep failure surface are common, while in plane areas, failure of raised embankment during occasional heavy or persistent rainfall has been very common [1]. This may happen due to various reasons which commonly include rainfall [2], earthquakes, snow melting [3], and rise in the groundwater table [4]. It has been observed that steep slopes are more vulnerable to failure than gentle ones mainly due to the angle of repose. Hence, to mitigate the slope failure, a thorough knowledge of the mechanics and process that regulates the slope's behavior is essential [5].

The embankments are one of the common type of civil engineering constructions using borrowed earth and artificial compaction. They are used as hydraulics structures, such as river and reservoir embankments, dykes, and waste containment structures. In transportation engineering such as road, railway embankments find the maximum applications. Their performance criteria are mostly determined by the reasons for which they are built. In hydraulics, seepage is the governing criterion, and in road and rail embankments, the settlement criterion and slope stability are the most important factors [6]. Embankment failure can occur in a variety of ways; for example, if the failure occurs near the surface of the slope in the form of gullying, it is referred to as shallow failure; however, if the failure occurs deep within the slope, causing the flow of chunks of soil, it is referred to as deep failure.

Railway embankments are generally significantly above the nearby ground level; hence, the water table usually does not interfere, and therefore, the embankment generally remains in unsaturated condition. However, during the monsoon season due to the rainfall, its soil may get into saturated condition and the groundwater if shallow then may reach the ground surface through capillarity. Usually water infiltrates from top or sideways into the railway embankments [7]. Several incidents of rainfall-induced catastrophes have been documented in India in the recent decade with numbers exceeding 2700 yearly, as per the Geological Survey of India [8]. Shear strength of certain soil is good enough in unsaturated condition but upon wetting their soil structure gets collapsed causing intensive damage to the property they are supporting [9]. In order to prevent such mishaps, embankments can be analyzed for different aspects of geotechnical engineering and need to be strengthened before plying of trains [10]. Rainfall infiltration is the primary cause of landslides, slope erosion, and collapse caving. All of these pose severe risks of loss to public and private property, economy, and life. Prevention from such untoward events which may cause damage can be minimized using various methods [11]. Specific and focused studies by many researchers have contributed by suggesting different mitigation methods, e.g., by observing effect of rainfall on slope stability [12–14]. Moreover, some studies have suggested that use of GIS could prove a vital tool to predict possible landslides areas [15].

This infiltration of the rain water into the embankment or rising of the phreatic level may lead to slope failure. In several regions of the world, rainfall induced slope collapse is a prevalent geotechnical risk. The impact of rainfall intensity and duration on slope stability has been established, whereas the reaction of unsaturated earth slopes to various rainfall circumstances is highly related to soil type. Among various other factors such as salinity [16], antecedent rainfall [17], it has also been found out that slope inclination is also one of the factor which influences failure of slope during rainfall [18]. Variability in rainfall pattern, intensity [19], duration, and the variation in behavior of different soil under partial and full saturation and submerged condition, make this issue complicated for geotechnical engineers. To overcome this problem, efforts to increase the stability of embankment, using different material and methods have evolved over time. Various techniques which involve reinforcing soil to increase the stability have been evolved over time. Some efficient materials used to reinforce soil are geo-composite [4], biopolymer

[20], jute [21], vetiver grass [22], geo-synthetics [1], and polyethylene terephthalate (PET). etc.

The angle of inclination of slope is the primary factor to be looked into as space constraints, sometimes lead to deviation from the well laid guidelines. If angle of slope inclination is kept as per the relevant codes, then other factors which affect the stability of slopes are to be looked into.

This study aims to investigate the slope failure on the railway embankment of the Dedicated Freight Corridor propose to run from Dadri to Kolkata in INDIA. The study was carried out just after 1 year of the embankment and rail track laying was completion, i.e., the year 2019–2020. During the field study, the main failure type observed over the slope was due to gullying at close intervals, there was diversity in the dimension of these gullies ranging from 0.4 m to as deep as 4.0 m and length ranging from 4 m to up to 15 m. The gullies many times braiding were formed after the embankment had already subjected to the full monsoon rain. The lab study was conducted through scaled physical modeling of the embankment. Further, numerical analysis has been carried out on GEO-STUDIO to evaluate the Factor of Safety in different conditions. In this study, we have analyzed embankment after every rainfall. Six gullies were reported during whole monsoon season. After every rainfall, dimensions of gullies (which was altering because of rainfall) were recorded. Numerical simulation was conducted on worst affected gullies (RG1 and CG4) of compacted and un-compacted portions after every rainfall. Dimension of gullies, which was changing after every other rainfall, was considered during performing numerical analysis. To get a clear behavior of embankment and its factor of safety against slope throughout rainy season, analysis was run for every deformation experienced by the embankment after every storm event.

Methods

A complete detailed study was done to analyze rainfall induced slope failure of railway embankment. Both scaled lab modeling and FEM based numerical analysis was done to achieve the goal of study. Prior to experimental modeling and numerical analysis, a field visit was done to have an overview of the gullies formed on railway embankment at site. Many gullies were found, and some of them were covered with turfing while others were not. Dimensions of four gullies were measured and tabulated in Table 3. Soil sample was also collected and requisite tests were performed in the lab. Experimental yard of Civil Engineering Department was chosen to prepare scaled lab model using the similar type of soil and scale factor of 1:25.33. Some part of the embankment was exposed to the natural vegetation to perform comparative study. In order to record the amount of rainfall rain gauge was placed near the lawn. Gullies formed as a result of rainfall, and their dimensions were recorded and tabulated for whole complete rainy season. A total of 12 gullies were recorded on the embankment as shown in the Fig. 11 (4 of them were present on the central uncompacted part while other 8 were formed on the compacted part. Moreover, FEM-based numerical analysis was performed using GEO-STUDIO. Morgenstern Price Method was utilized among all other available methods of limit equilibrium methods. Factor of safety of model's embankment was calculated at worst affected sections (RG1 and CG4) after every rainfall. As the dimensions of gullies were changing after every rainfall, numerical analysis was performed for every changed configuration.

Maximum depth of gully was incorporated in the numerical analysis by assuming total depth of gully to be at central part of slope.

Field details

Project details

The Indian economy has been growing and is expected to increase in the future, creating the need for new rail freight transit capacities. This growing need led to the laying of the freight corridors along the East and West routes. The Ministry of Railways took steps to create a Special Purpose Vehicle to oversee the building, operation, and maintenance of dedicated freight routes. As a result, the "Dedicated Freight Corridor Corporation of India Limited (DFCC)" was formed on October 30, 2006, under the Companies Act 1956, to design and build dedicated freight corridors, mobilize financial resources, and construct, maintain, and operate them. Six freight routes will be built across the country as part of this project. Routes of corridor which has been sanctioned and are yet to be sanctioned are shown in Fig. 1. The project's goal is to build a freight transportation system that is both safe and efficient. The Western DFC, which connects the states of Haryana and Maharashtra, and the Eastern DFC, which connects the states of Punjab and West Bengal, are the first two freight corridors to be built. The Western and Eastern DFCs have a total length of 2843 km. The project's overall cost is expected to be $11.38 billion. The 1873 km Eastern Dedicated Cargo Corridor consists of 2 distinct segments: a 1426 km electrically powered two-track segment from Dankuni, West Bengal to Khurja, Uttar Pradesh, and a 447 km electric one-track segment Khurja—Dadri, UP to Ludhiana, Punjab. The Western Dedicated Freight Corridor runs from Jawaharlal Nehru Port Trust, Navi Mumbai, Maharashtra to Dadri UP, through Vadodara-Ahmedabad-Palanpur-Phulera-Rewari over a length of 1504 km of double line electric (2×25 VK) rail. With the exception of Diva, Surat, Ankleshwar, Bharuch,Vadodara, Anand, Ahmedabad, Palanpur, Phulera, and Rewari, the course has been preserved parallel to current lines [23].

Field observations at chosen section

In this study, a detailed study of the recently laid embankment was carried out at Wair, Badshahpur of Noida, 90 km from the capital city of Delhi. Location using google maps showing our presence at the site. The dimensions of the embankment were provided by the concerned authority as tabulated in Table 1. Different morphological parameters were measured using field clinometers.

Some soil properties (maximum dry density and optimum moisture content) were provided by the authority while other relevant tests were performed in labs at the Department of Civil Engineering as mentioned in Table 2. Observations made at the lab were used to compute the properties of soil using different methods in Fig. 2.

There were many cutting/gullying failures along the embankments. Measurements of 4 gullies were done using tape in which two of them were covered with vegetative turf and two others which were barren as shown in Figs. 3, 4, 5, and 6. Details of these measurements are tabulated in Table 3.

Fig. 1 Map of the DFCCIL Project [30]

Table 1 Physical details of embankment

S. no	Features	Dimension
1	Base width	38 m
2	Top width	10 m
3	Total height	7 m
4	Side slope	1 V:2H

Lab modeling

Model details

A lab model of the actual embankment was constructed at a reduced scale of 1:25.33 in the testing yard of the Department of Civil Engineering, Z.H.C.E.T., AMU, Aligarh,

Table 2 Properties of soil derived from chosen section and one used in making model

S. No	Properties	Values	
		Chosen section	**Model**
1	Dry density of embankment's soil	1.55gm/cc	1.53gm/cc
2	Maximum dry density	1.88gm/cc	1.84gm/cc
3	Optimum moisture content	10.22%	11.22%
4	Plastic limit	19%	19%
5	Liquid limit	24%	22%
6	Specific gravity	2.6	2.67
7	Cohesion	45 kPa	54
8	Angle of friction	9.80^0	11.58^0
9	Type of soil	CL-ML	CL-ML

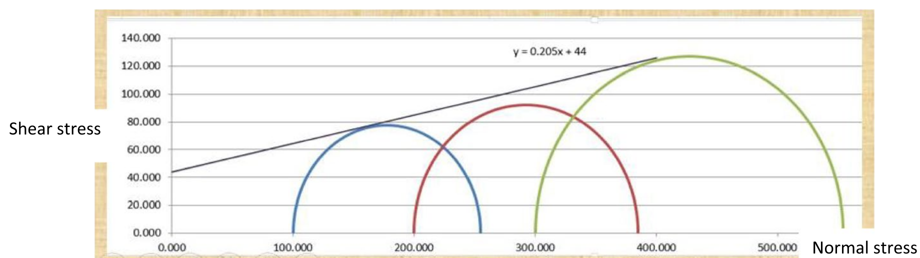

Fig. 2 Mohr's Failure Envelope

Fig. 3 Studied embankment at Wair, showing effect of gullying and slope failure no 1

Fig. 4 Studied embankment at Wair, showing effect of gullying and slope failure no 2

Fig. 5 Studied embankment at Wair, showing effect of gullying and slope failure no 3

India. Cross-sectional details using drawings and real-life images are shown in Figs. 7 and 8, and physical dimensions are tabulated in Table 4.

Similar soil was chosen for the embankment model. First, a well-compacted subgrade was created through ramming and then the embankment was raised in 3 layers, compacting each layer at OMC. In the model, the side slopes were well compacted during the construction of the model while the lateral slopes were comparatively less compacted. To compare the gullying on non-turfed with that of turfed slopes, the middle portion of 1 m on each side of the embankment was covered with grass and Portulaca plant (to replicate

Fig. 6 Studied embankment at Wair, showing effect of gullying and slope failure no 4

Table 3 Description of failure patterns

S. No	Features	Dimensions			
		Failure no. 1	Failure no. 2	Failure no. 3	Failure no. 4
1	Turfing	Not present	Not present	Not present	Not present
2	Length	15.0 m	4.0 m	15.0 m	3.1 m
3	Width	1.1 m	0.8 m	3.5 m	0.6 m
4	Depth	4.0 m	0.4 m	4.0 m	0.8 m
5	Failure Pattern	Inclined over slope	Straight	Inclined over slope	Zig-Zag

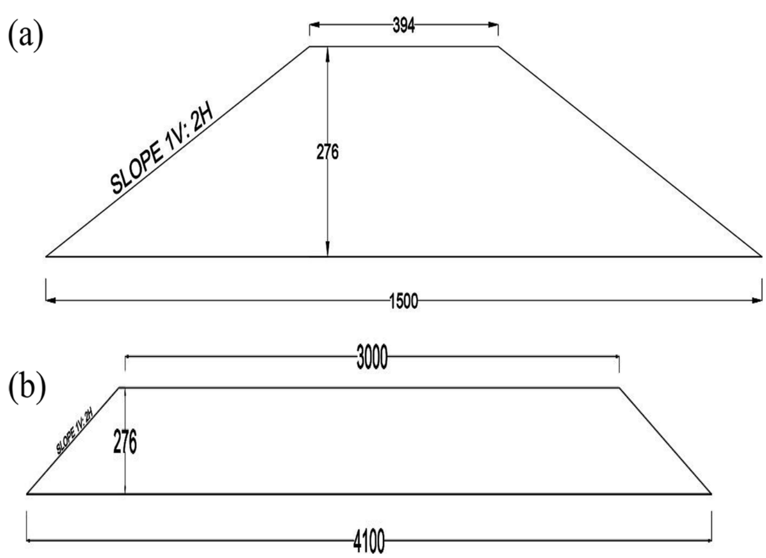

Fig. 7 **a** Lateral Cross-Sectional Details of Model (all dimensions in mm). **b** Longitudinal Cross-Sectional Details of Model (all dimensions in mm)

Fig. 8 a, b Cross-sectional details of fully constructed embankment

Table 4 Dimension of the lab model

S. No	Features	Dimensions
1	Total length	4100 mm
2	Base width	1500 mm
3	Top width	394 mm
4	Total height	276 mm
5	Side slopes	1 V:2H

Fig. 9 Grass placed over a length on both sides of compacted embankment

vegetative turf surface) as shown in Fig. 9. Coarse aggregate was placed on the top surface of the model to incorporate the effect of rail ballast on the actual embankment.

The work was carried out from 12 July 2021 to 11 September 2021 which has seen the natural rainfall in the monsoon season. For the measurement of rainfall over the model, a manual rain-measuring gauge was placed near it. After constructing the embankment, the onsite dry density of the embankment was calculated with the help of mini core cutter apparatus.

Soil properties

After conducting several tests on embankment soil as per the Indian Standard method of testing, the following properties were observed (Table 2). Mohr's failure envelope was drawn as shown in Fig. 10 to compute cohesion and angle of friction.

Observation of model embankment's dimensions under rain and vegetation

Details of the gullies formed after every rainfall was recorded and was named to make our study informative and easy to understand for the one going through it. Names given to the gullies formed are illustrated in the following animated 3D figure as shown in Fig. 11.

Observations of rain fall induced failure of model

On the 12th of July, light rainfall of 4.4 mm was observed to which our embankment showed perfect resistance which is obvious from Fig. 12a, b. Another rainfall of 3 mm was observed on 17th July, and the response of the embankment remains the same as shown in Fig. 13.

Rainfall amounting to 53 mm was recorded on the 20th of July which causes damage to the central less compacted part of the embankment. A gully of 4 cm width and 4 cm deep (named CG1) was observed as conveyed in Fig. 14. Merely after 2 days, i.e., 22nd of July, rainfall amounting to 68 mm was recorded. This rainfall proved fatal to the embankment as 6 more new gullies were formed. Two of them were on the left-hand side of the longitudinal slope (LG3 and LG4) as depicted in Fig. 15(a), and another two were formed on the right-hand side of the longitudinal slope (RG1 and RG2) as shown in Fig. 15b, while another two were observed on central less compacted part (CG3 and CG4) as depicted in Fig. 16. Dimensions of gullies were regularly recorded and updated from time to time as shown in supplementary documents. Continuous rainfall for

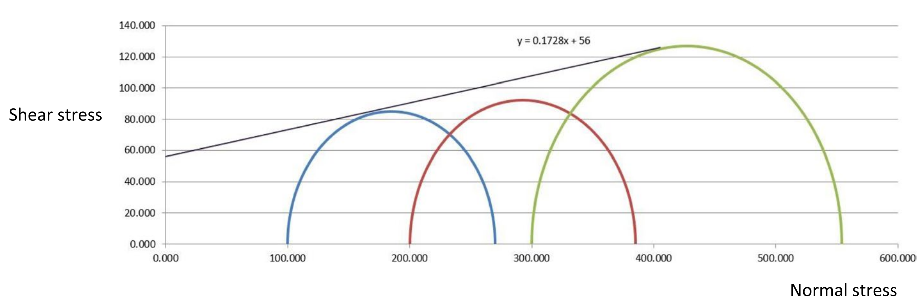

Fig. 10 Mohr's Failure Envelope

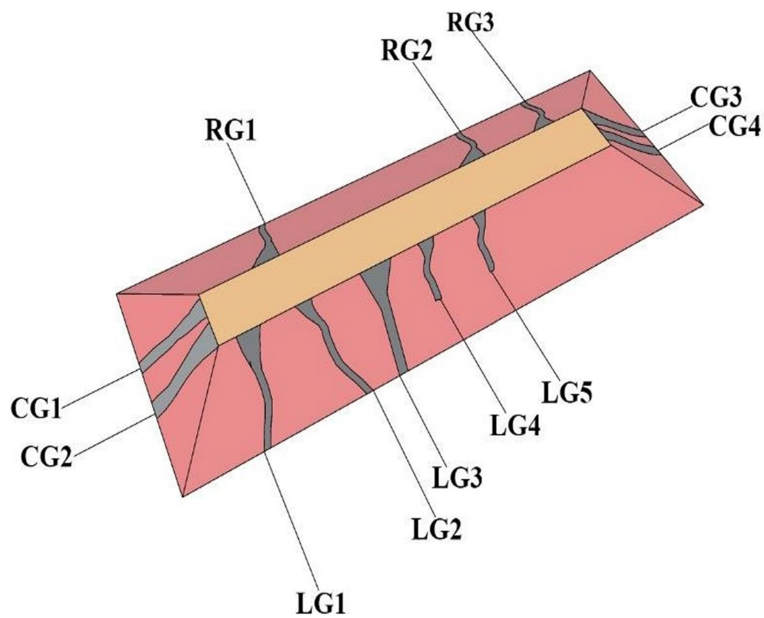

Fig. 11 Illustration of the embankment showing the final gullies after one rainy season

Fig. 12 **a, b** Depicting perfect resistance shown up by embankment against gullying

two consecutive days amounting to 54 mm was observed on the 27th and the 28th of July. This storm leads to the formation of another two new gullies (named as LG2 and CG2) as depicted in Fig. 17a, b. Little change was observed in the previous formed gullies. Another storm of 25 mm was recorded on the 29th and 30th of July which causes another two new gully formations (LG1 and RG3).

Little rainfall of 4 mm on the 2nd of August was observed which causes little change in previously formed gullies. A significant amount of vegetation was observed as depicted in Fig. 18. A very light intensity of rainfall was observed on the 20th and 21st of August and was unable to change the dimension of the embankment. Rainfall amounting to 60 mm on the 31st of August was observed and was unable to distort the configuration of the embankment. Significant vegetation cover was observed on the 31st of August as shown in Fig. 19. Continuous rainfall amounting to 80 mm during the 2nd and 3rd of September was recorded which causes very little or no change

Fig. 13 Depicting no gully formation even after second rainfall

Fig. 14 Shows gully formation at less compacted central face of embankment

in the dimension of previously formed gullies suggesting the effect of hydro-compaction and increasing vegetal growth. The last recorded rainfall amounts to 70 mm was recorded between 8 and 11 September which causes a minute change in the central less compacted part and no change in the compacted part.

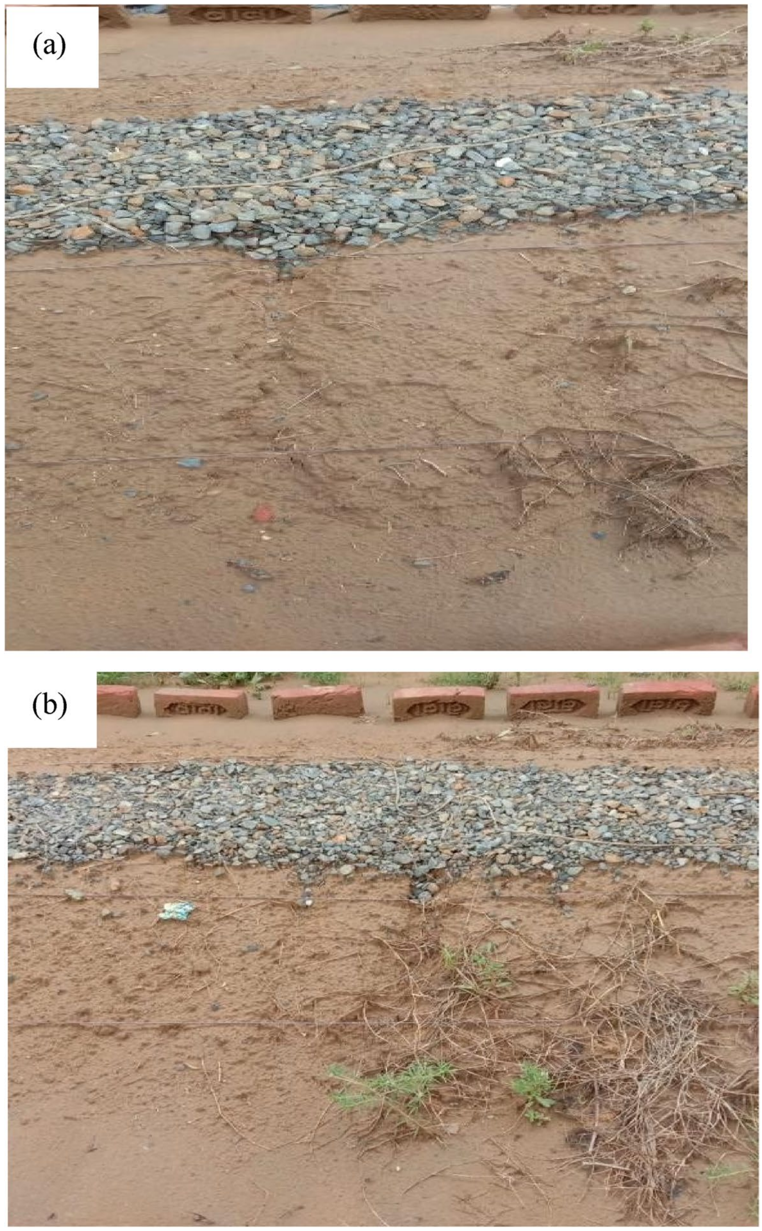

Fig. 15 a Conveying two new gullies on left side of longitudinal slope. **b** Conveying two new gullies on right side of longitudinal slope

Discussion of experimental study

During the whole rainy season, the minimum rainfall observed was 3 mm while the maximum rainfall of 80 mm was recorded. On an average, the scaled model has faced 40.127 mm of rainfall throughout the rainy season. In terms of the total rainfall, the model encountered 441.4 mm during the whole rainy season. As a result of rainfall model undergoes deformation in the form of gullies which were measured after the occurrence of every rainfall. The compacted portion RG1 stood strong and did not show up any deformation till the fourth rainfall, after which the gully was observed at 0.0724 h depth (where h is the total height of the scaled model, i.e., 276 mm). At the end of the

Fig. 16 Showing two newly formed gullies on lateral side

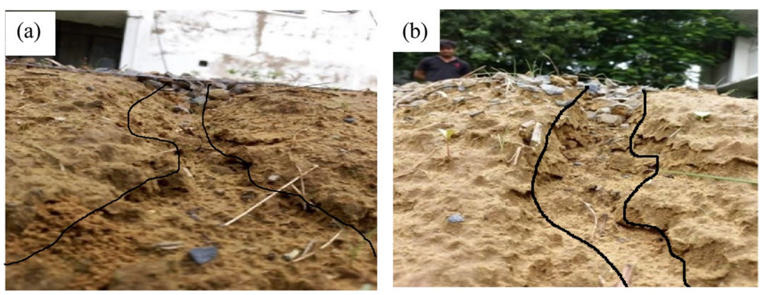

Fig. 17 **a** Depicting a new gully on left hand side of embankment. **b** Showing a new gully formed on less compacted central portion of embankment

rainy season, RG1 reported a maximum gullying of 0.199 h. Less compacted CG4 also showed up resistance to the failure till the fourth rainfall after which it gets eroded by 0.217 h. The maximum depth of the gully measured for the same at the end rainy season was 0.688 h.

Numerical analysis

Modeling details

A series of numerical simulations have been carried out on GEOSTUDIO 2016 to observe the effect of the degree of compaction and rainfall cycle. The main result of the analysis was to calculate the Factor of Safety (FOS) of the embankment's slope under changing rainfall conditions. The simulation was performed on both less and

Fig. 18 Shows growth of vegetation on embankment

Fig. 19 Shows significant cover of vegetation over embankment

well-compacted parts of the embankment. As multiple gullies were observed on less and well-compacted, simulation was performed on the worst affected gullies (CG4 and RG1).

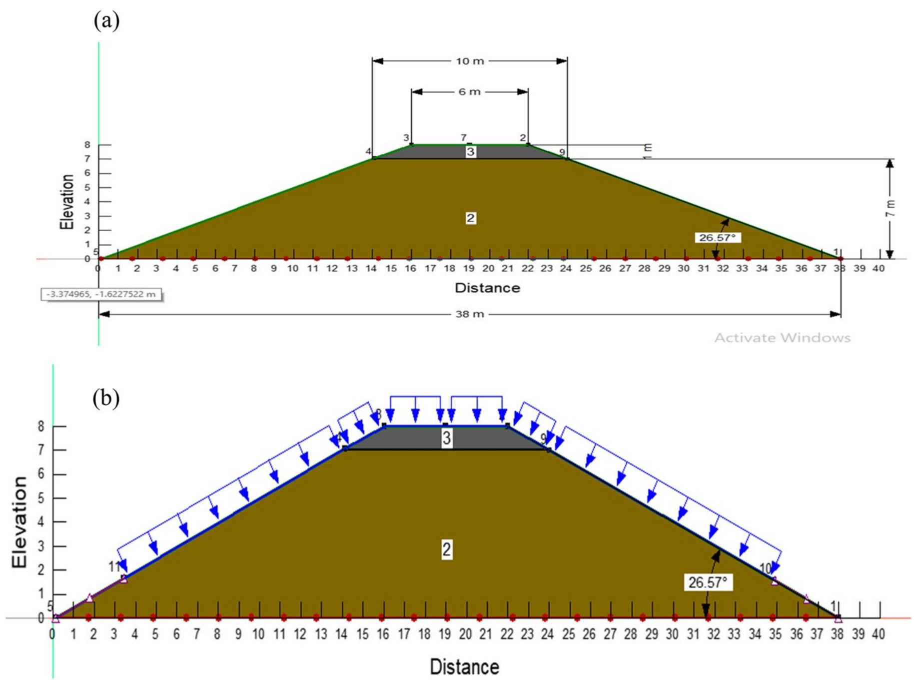

Fig. 20 **a** Dimensions of the Geo-Studio Model. **b** Boundary layers conditions of the model

Table 5 Scaled up depth of gullies at RG1 and CG4

S.No	Depth of gully before scaling up(cm)	Depth of gully after scaling up (m)
1	2	0.5
2	4	1.01
3	5.5	1.39
4	6	1.52
5	7	1.773
6	12	3.04
7	15	3.8
8	19	4.81

To incorporate the effect of rainfall on the slope stability in the study, sequential analysis has been performed. A seepage analysis through SEEP/W was followed up by SLOPE/W for the determination of FOS at that particular rainfall.

The dimension of the embankment and gullies was scaled up to the actual embankment size, and then, the model was created as shown in Fig. 20a. The scaled-up depths of gullies were summarized in Table 5.

The layer of gravel of 1 m height was also created over the embankment, to incorporate the effect of rail ballast which is present in actual railway embankments.

First, the finite element-based seepage analysis using the SEEP/W was conducted in which seepage condition was assumed. A grid size of 0.6 m was chosen for the FEM analysis. It was observed that the results were improving, and computational time was increasing as mesh size was reduced. Since 0.6 m was the optimum size of the grid available, therefore this size was utilized to perform numerical analysis. The amount of rainfall showered over the model was recorded and utilized in determining the rainfall intensity. This intensity was used to perform numerical analysis by projecting the calculated intensity over the embankment. The boundary condition at the base of the embankment was chosen as at zero pressure, whereas the top of the embankment was fixed for the rainfall boundary condition.

For the slope, the length of the embankment was divided into 5 parts where 4/5 of its length was fixed for rainfall and the rest length at the bottom was fixed as the drainage boundary condition as shown in Fig. 20b.

Further after conducting the seepage analysis, the slope stability analysis was carried out, using the SLOPE/W analysis considering the submerged condition from the SEEP/W analysis. For the SLOPE/W analysis, Morgenstern Price Method of Limit Equilibrium Method was adopted. The FOS for the critical slip surface was recorded for results.

Simulations and results

For performing numerical simulation, we have divided the work into the following cases as detailed below:

Case 1: Simulation on well-compacted side

a FOS of embankment without considering any geometric deformation

The stability of the embankment was tested several times in both dry and submerged conditions. The embankment was found to be stable using SLOPE/W analysis on GEO-STUDIO, with a factor of safety of 2.764, indicating a stable construction (as depicted in Fig. 21a). The seepage study of the model under 1.66E − 5 m/s rainfall infiltration shows the formation of a critical surface near the sloping portion which demonstrates the possibility of surface failure/gullying failure. The factor of safety registered by GEOSTUDIO under steady seepage conditions was 0.477 as shown in Fig. 21b.

b FOS of embankment considering gullies formation after every rainfall

The initial 0.5 m gullying occurred during the second rainstorm of intensity 1.88E − 05 m/s, with a factor of safety of 0.306 recorded by GEO STUDIO as shown in Fig. 22a. Furthermore, additional rainfall with an intensity of 1.66E − 05 m/s damages the embankment even more by causing 1.01 m gullying. Using software, a factor of safety of 0.362 was found under steady seepage conditions which are depicted in Fig. 22b. After the occurrence of rainfall with an intensity of 2.20E − 05 m/s, the greatest gullying of 1.39 m was discovered. The software calculated a factor of safety of 0.287 in this instance as shown in Fig. 22c.

c FOS variation over the deformed and undeformed embankment by varying the rainfall intensity

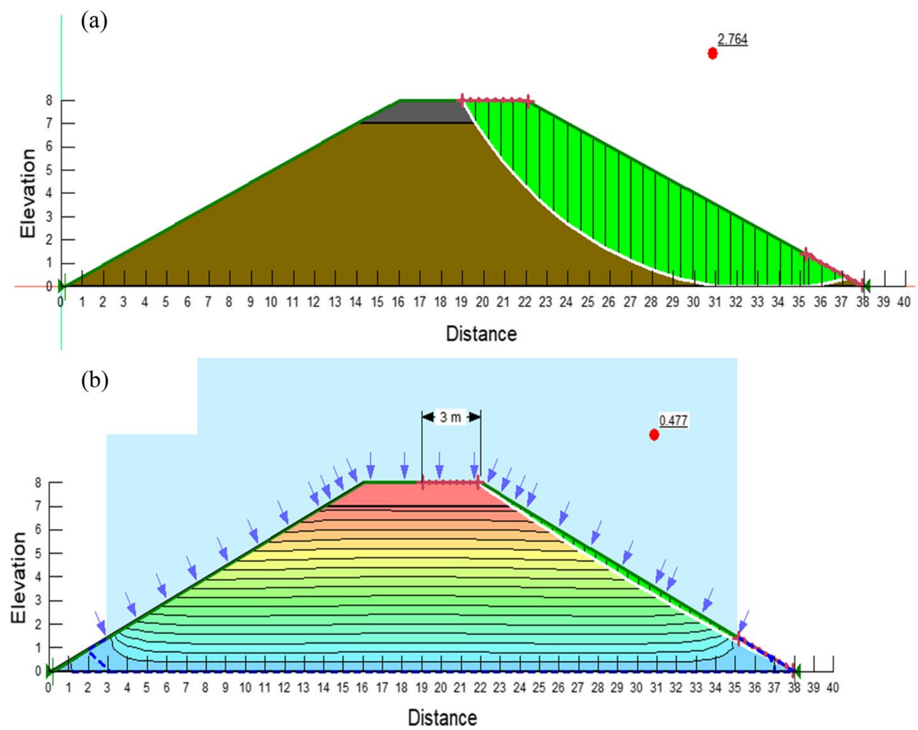

Fig. 21 **a** FOS of embankment without rainfall. **b** FOS at RG1 with maximum rainfall

Through software simulation, the effect of increased rainfall intensity on FOS of the highest reported gullying (1.39 m) of the embankment and undeformed embankment was also evaluated. FOS showed a decreasing tendency as rainfall intensity rose for both cases which are clearly visible in Fig. 23. However, as the intensity of rainfall increased, the decremental decrease in each iteration decreased. FOS was 0.375 at a rainfall intensity of 20 mm/h, dropping to 0.360 at 160 mm/h for deformed gullying. Similarly, for the original embankment, FOS at 20 mm/h was observed as 0.45 which drops to 0.422 at 160 mm/h.

Case 2: Simulation on a less compacted side

a FOS of embankment without considering any geometric deformation

In this case, stability was checked for submerged conditions under the influence of maximum rainfall, i.e., 80 mm recorded during the entire period. The embankment was unstable as GEO-STUIDO showed up a factor of safety of 0.597 as shown in Fig. 24a. Moreover, the critical surface formed was nearby the top surface, indicating the proneness of this part of the embankment to shallow failure in the form of gullies.

b FOS of embankment considering gullies' formation after every rainfall

In the central part of the embankment which was less compacted, four gullies formation were observed throughout the data recording period. The gully which deformed

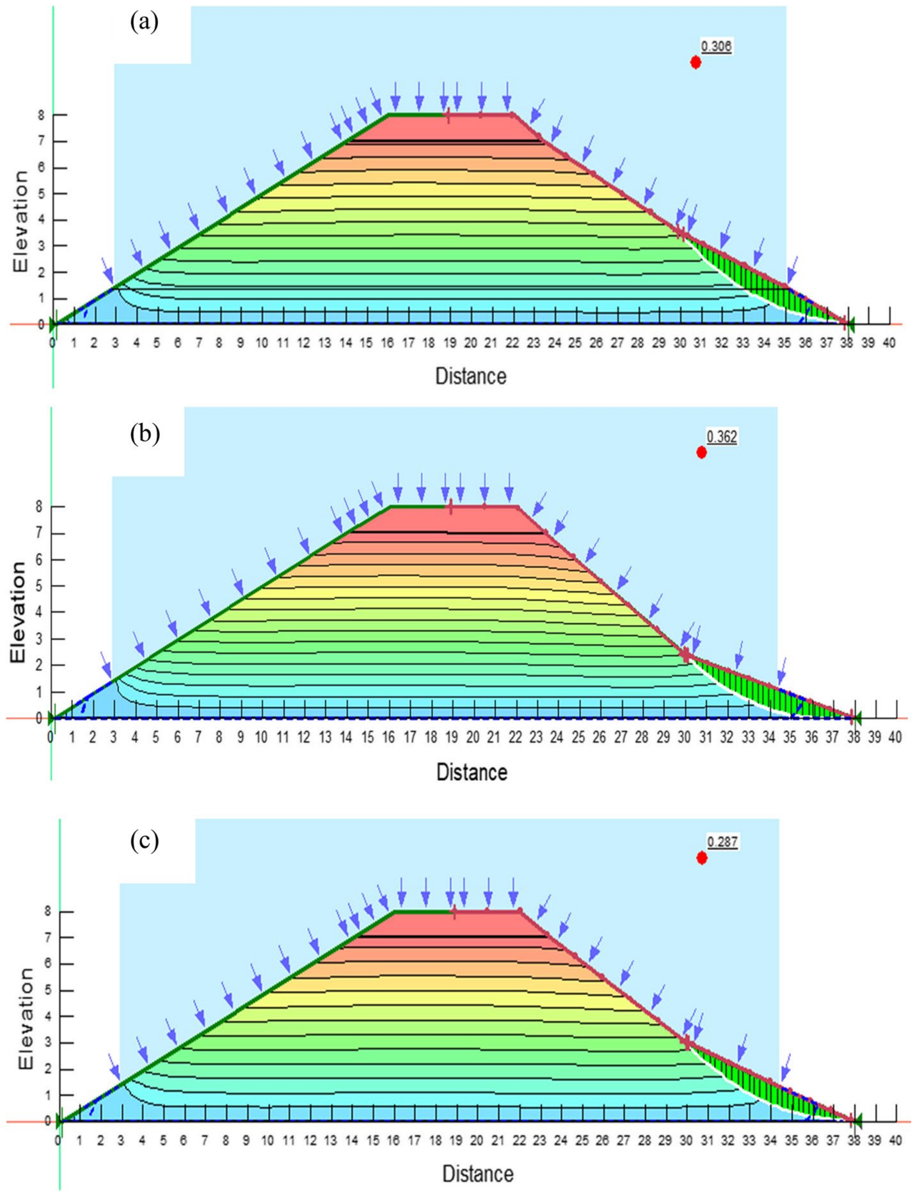

Fig. 22 **a** FOS at RG1 with 2 cm gully for 68 mm rainfall. **b** FOS at RG1 with 4 cm gully for 60 mm rainfall. **c** FOS at RG1 with 5.5 cm gully for 80 mm rainfall

and destructed most due to rainfall was CG4. Considering CG4 as a critical one, we have performed numerical simulations on this gully only.

The FOS registered by GEO-STUDIO for initial deformation of 1.52 m with rainfall intensity of 1.88E − 05 m/s was 0.691 as shown in Fig. 24b. The second storm which struck the lab model was just after 5 days and it changed the depth of gully to 1.773 m. After being analyzed through steady-state analysis, this gully which faced rainfall intensity of 1.5E − 05 m/s showed up the very same FOS as of the last case, i.e., 0.691 as shown in Fig. 24c. The third storm affected CG4 severely and caused the deformation of 3.04 m. The rainfall intensity for this storm was found to be 1.66E − 05 m/s. After performing analysis, the factor of safety got reduced by 11% to 0.610 as shown in Fig. 25a. Another

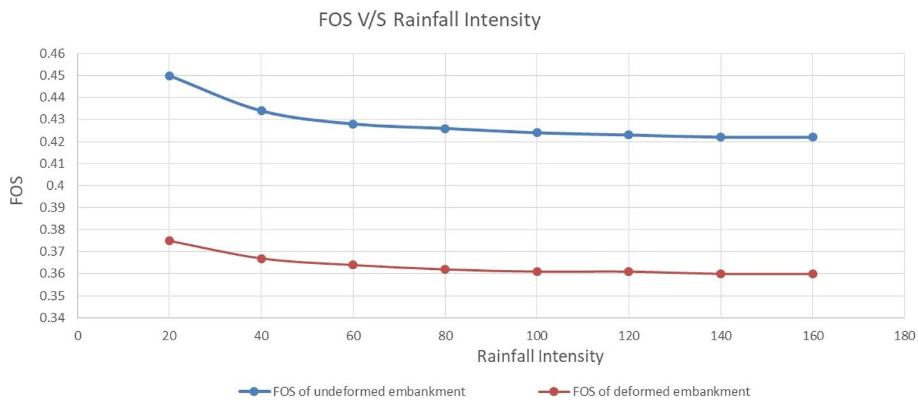

Fig. 23 FOS variation over the deformed and undeformed by varying the rainfall intensity

storm of intensity 2.2E − 05 m/s deteriorate the slope further by increasing the depth of gullying to 3.8 m. Slope stability analysis under steady-state analysis in GEO-STUDIO recorded a factor of safety of 0.544 as shown in Fig. 25b. The depth of the gully recorded was 4.81 m after the occurrence of previous rainfall and rainfall intensity observed in this storm was 1.66E − 05.GEO-STUDIO shows a factor of safety of 0.279 for this case as shown in Fig. 25c. As compared to the last scenario, it can be said that FOS drops drastically this time by 54%. Since FOS was less than in each case, it can be concluded that the central part of the embankment (CG4) was not stable at all. Moreover, as the embankment was getting deformed under the effect of rainfall, and FOS was also getting reduced.

Results and discussion

This study included a detailed scaled lab modeling and numerical analysis. Gullies' observation during the whole monsoon season showed that vegetation cover provides reinforcement to the embankment and stabilizes it. Moreover, the part which was less compacted suffered much higher deterioration than the compacted part. Morgenstern Price Method was chosen among all limit equilibrium methods to run numerical analysis on GEO-STUDIO. Thorough numerical analysis was done for RG1 and CG4 after every storm event incorporating the effect of changing cross-section. A decreasing trend of FOS was recorded for both RG1 and CG4 after every storm event. It was also seen that FOS reduced with an increase in rainfall intensity and becomes constant after reaching a particular value.

Conclusions

Failure of slope in the form of settlement, gullying, spalling, or surface slip failure is a very common phenomenon, especially during the rainy season. To analyze the effect of rainfall on the railway embankment, a thorough study through both lab modeling and numerical analysis were carried out.

It was observed that under the influence of rainfall the section of the embankment which was well compacted as per codal standards, experienced less damage as compared to the less compacted part of the embankment. The maximum depth of the gully observed for the compacted part was 0.199 h (0.199 times the height of the

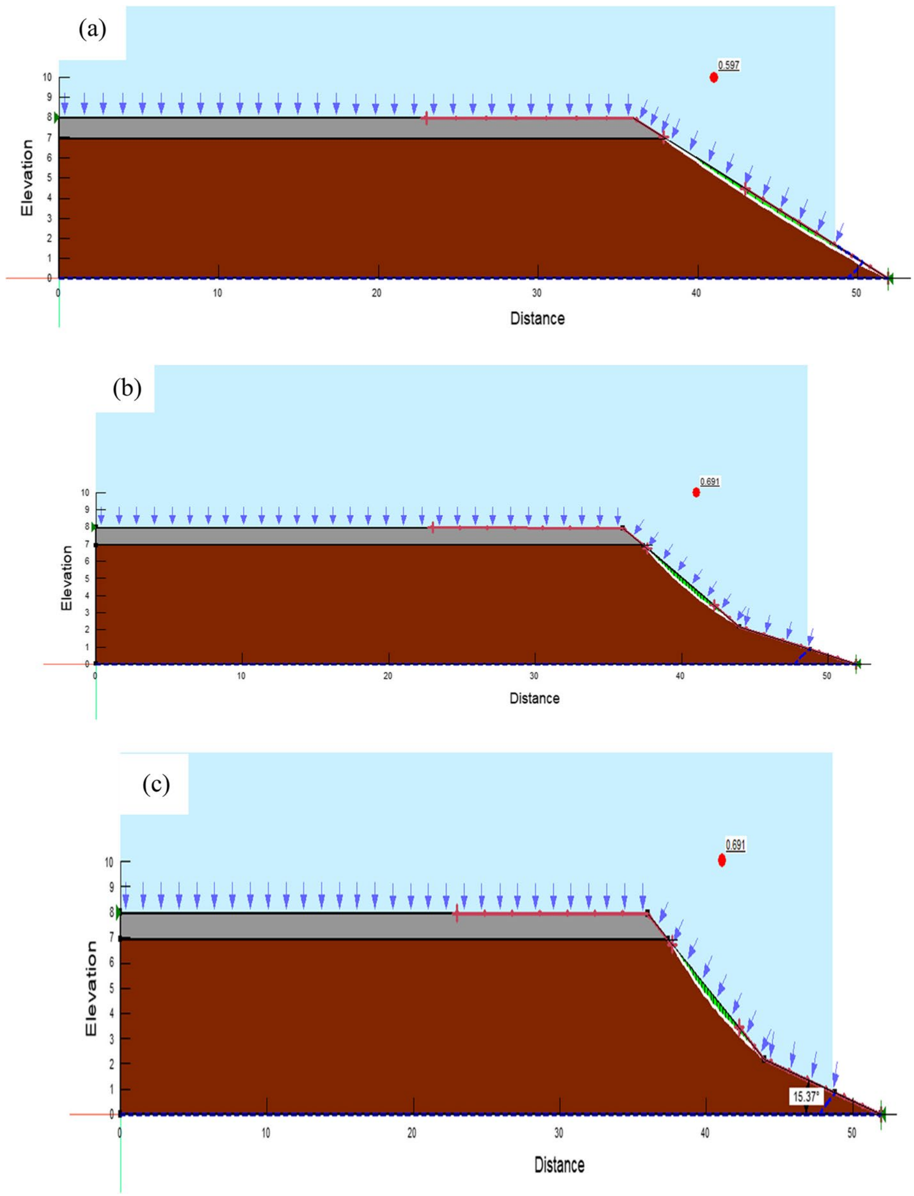

Fig. 24 **a** FOS of longitudinal section of embankment under the influence of maximum rainfall recorded. **b** FOS at CG4 with 7 cm gully for 54 mm rainfall. **c** FOS at CG4 with 7 cm gully for 54 mm rainfall

embankment), while the less compacted part suffered heavy surface erosion and got inflicted with a gully depth of 0.688 h. Vegetation cover provides safety from direct rain impact as well as resistance to embankment erosion and surface failure by root anchoring. The embankment covered with vegetation showed up the marked differences with lesser and shallower gullies as compared to other non-vegetative parts.

The numerical simulations were performed on the cross-section having the worst affected gullies of both well-compacted and less compacted parts region (RG1 and CG4, respectively). Further, the change in cross-sections has been incorporated in every analysis explicitly for each rainfall. In the simulation of maximum rainfall on initial embankment cross-sections, the FOS was less than one in both regions. With an increase in

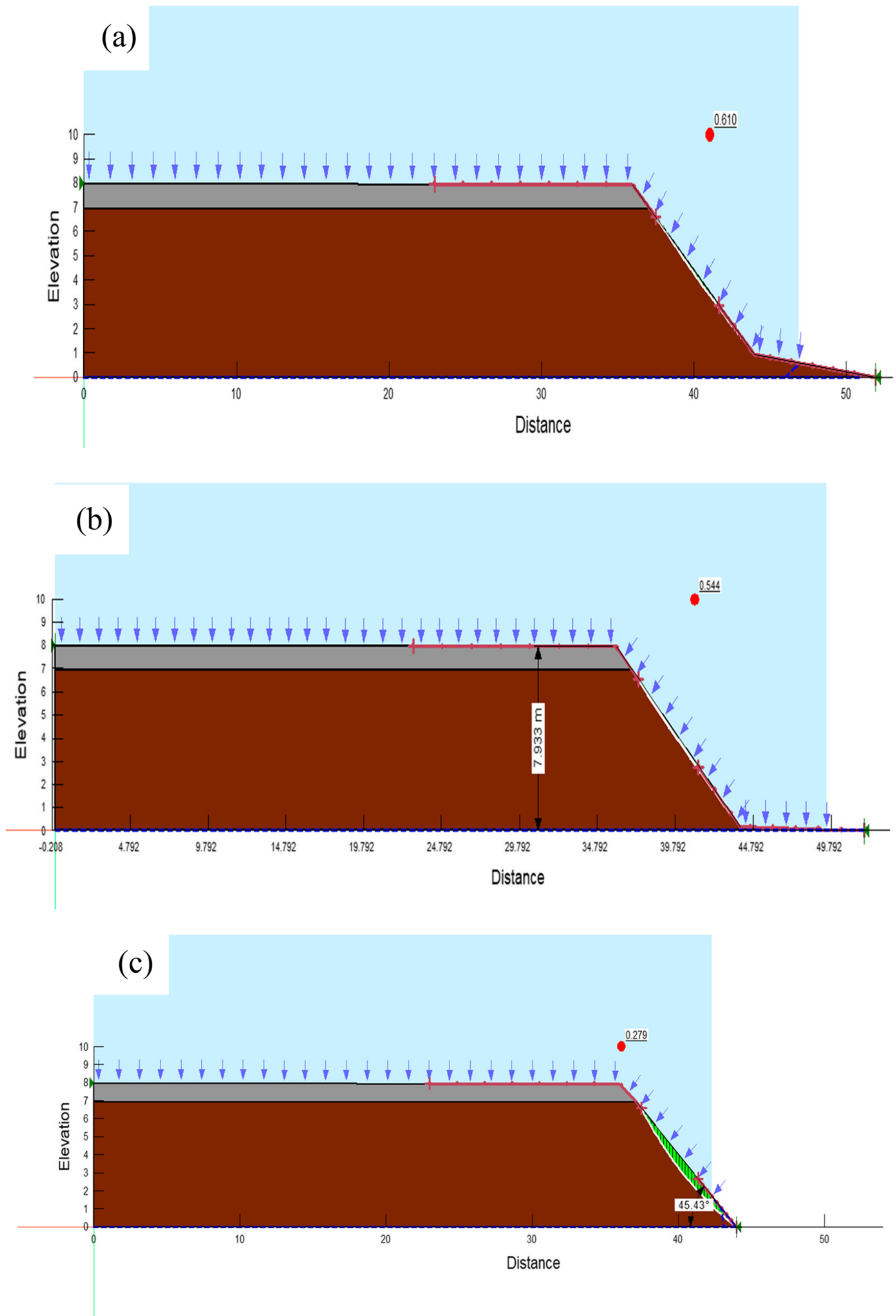

Fig. 25 **a** FOS at CG4 with 12 cm gully for 60 mm rainfall. **b** FOS at CG4 with 15 cm gully for 70 mm rainfall. **c** FOS at CG4 with 19 cm gully for 80 mm rainfall

rainfall, the FOS decreases up to 100 mm, then no significant change has been observed. However, the presence of a gully has further weakened the FOS. It clearly indicates that FOS calculated in normal conditions is too higher than the actual FOS after the rainfall. Moreover, it becomes important to crucially analyze the FOS of such embankments carrying high-speed freight trains. Hence, it has been recommended that immediate safety measures are necessary to mitigate the failure and avoid accidents, especially for high-speed trains.

Abbreviations

FOS	Factor of safety
h	Total height of the embankment
FEM	Finite element method
RGx	Gully appeared on the right side of the embankment
LGx	Gully appeared on the left side of the embankment
CGx	Gully appeared on the central side of the embankment

Acknowledgements
We would like to express our special thanks of gratitude to our Civil Engineering Department, Aligarh Muslim University, for facilitating experimental and numerical work.

Authors' contributions
Mohammad Aqib (MA), Shadab Usmani (SU), Tanveer Khan (TK), Md Rehan Sadique (MRS), Mohd Masroor Alam (MMA). The idea and conceptualization of the study were made by authors TK, MRS, and MMA. Field study were carried out by MA and SU under guidance of TK. The experimental and numerical analysis were carried out by MA and SU under supervision of MRS and MMA. The preparation of the manuscript was carried out by author MA and SU, and expert suggestions were provided by MRS and MMA. The final version of the manuscript was approved after each author's (ALL) detailed editing and evaluation. The authors have read and approved the final manuscript.

Funding
The authors declare that they have not received any financial aid from any source in this study.

Availability of data and materials
The datasets generated and analyzed during the current study are available in the manuscript and attached files of tables and figures.

Declarations

Competing interests
The authors declare that they have no competing interests.

Received: 15 October 2022 Accepted: 28 February 2023
Published online: 15 March 2023

References

1. Bhattacherjee D, Viswanadham BV (2015) Numerical studies on the performance of hybrid-geosynthetic-reinforced soil slopes subjected to rainfall. Geosynth Int 22(6):411–427
2. Regmi RK, Jung K, Nakagawa H, Do XK, Mishra BK (2017) Numerical analysis of multiple slope failure due to rainfall: based on laboratory experiments. CATENA 150:173–191
3. Mori A, Subramanian SS, Ishikawa T, Komatsu M (2017) A case study of a cut slope failure influenced by snowmelt and rainfall. Procedia Eng 189:533–538
4. Bhattacherjee D, Viswanadham BV (2018) Effect of geocomposite layers on slope stability under rainfall condition. Ind Geotech J 48(2):316–326
5. Kayal JR, Zhao D, Mishra OP, De R, Singh OP (2002) The 2001 Bhuj earthquake: tomographic evidence for fluids at the hypocenter and its implications for rupture nucleation. Geophys Res Lett 29(24):5–1
6. Cheuk CY, Ng CW, Sun HW (2005) Numerical analysis of soil nails in loose fill slopes subjected to rainfall infiltration effects. Comp Geotech 32:290
7. Wang YX, Guo PP, Shan SB, Yuan HP, Yuan BX (2016) Study on strength influence mechanism of fiber-reinforced expansive soil using jute. Geotech Geol Eng 34:1079–1088
8. Huang L, Wu C, Wang B, Ouyang Q (2018) A new paradigm for accident investigation and analysis in the era of big data. Process Safety Prog 37(1):42–48
9. Opukumo AW, Davie CT, Glendinning S, Oborie E (2022) A review of the identification methods and types of collapsible soils. J Eng Appl Sci 69(1):1–21
10. Xu S, Zsáki AM (2021) (2021) Maximum safe freight train speed on railway embankments under rapid drawdown conditions based on coupled stress-seepage slope stability analysis. Transp Geotech 27:100486
11. Steinberg ML (1998) Geomembranes and the control of expansive soils in construction. McGraw-Hill, New York
12. Wu W, Berhe TG, Ashour T. (2012) Embankments and dams. InModern Earth Buildings 2012 Jan 1 (pp. 538–558). Woodhead Publishing. https://doi.org/10.1533/9780857096166.4.538
13. Lee LM, Gofar N, Rahardjo H (2009) A simple model for preliminary evaluation of rainfall induced slope instability. Eng Geol 108:272–285
14. Hossain J, Hossain MS, Hoyos LR. (2013) Effect of rainfall on stability of unsaturated earth slopes constructed on expansive clay. InGeo-congress 2013: stability and performance of slopes and embankments III 2013 (pp. 417–425). https://doi.org/10.1061/9780784412787.042

15. Yunus MZ, Ahmad FS (2016) GIS technology as a tools to predict landslide. ARPN J Eng Appl Sci 11(4):2581–2586
16. Kolahdooz A, Sadeghi H, Ahmadi MM. (2020) A numerical study on the effect of salinity on stability of an unsaturated railway embankment under rainfall. InE3S Web of Conferences 2020;195;01004). EDP Sciences. https://doi.org/10.1051/e3sconf/202019501004
17. Rahardjo H, Li XW, Toll DG, Leong EC. (2001) The effect of antecedent rainfall on slope stability. InUnsaturated soil concepts and their application in geotechnical practice 2001 (pp. 371–399). Springer, Dordrecht. ISBN: 978-94-015-9775-3
18. Gallage C, Jayakody Arachchige SP, Uchimura T. (2012) Effects of slope inclination on the rain-induced instability of embankment slopes. InProceedings of the second international conference on geotechnique, construction materials and environment 2012 (pp. 196–201). The GEOMATE International Society. ISBN: 978-4-9905958-1-4
19. Lin H, Zhong W (2019) Influence of rainfall intensity and its pattern on the stability of unsaturated soil slope. Geotech Geol Eng 37(2):615–623
20. Caballero S, Acharya R, Banerjee A, Bheemasetti TV, Puppala A, Patil U (2016) Sustainable slope stabilization using biopolymer-reinforced soil. InGeo-Chicago 2016:116–126
21. Sengupta A, Kumar S. (2012) Study of a model slope reinforced with jute. In Recent Advances in Modeling Landslides and Debris Flows 2015 (pp. 289–305). Springer, Cham. https://doi.org/10.1007/978-3-319-11053-0_24
22. Islam MS, Shahriar BA, Shahin HM (2013) Study on growth of vetiver grass in tropical region for slope protection. GEOMATE J 5(10):729–734
23. DFCCIL official website. https://dfccil.com.